www.czasopisma.pan.pl PAN www.journals.pan.pl
Opto-Electronics Review 26 (2018) 29–34

Contents lists available at ScienceDirect

Opto-Electronics Review

journal homepage: http://www.journals.elsevier.com/opto-electronics review

Self-swept erbium fiber laser around 1.56 μm

P. Navratil[a,b,c,*], P. Peterka[a], P. Vojtisek[a,d], I. Kasik[a], J. Aubrecht[a], P. Honzatko[a], V. Kubecek[b]

[a] Institute of Photonics and Electronics of the Czech Academy of Sciences, Chaberska 57, 182 51 Prague, Czechia
[b] Faculty of Nuclear Sciences and Physical Engineering, Czech Technical University in Prague, Brehova 7, 115 19 Prague, Czechia
[c] Currently with HiLASE Centre, Institute of Physics of the Czech Academy of Sciences, Za Radnici 828, 252 41 Dolni Brezany, Czechia
[d] Currently with TOPTEC Centre, Institute of Plasma Physics of the Czech Academy of Sciences, Sobotecka 1660, 511 01 Turnov, Czechia

ARTICLE INFO

Article history:
Received 28 September 2017
Accepted 28 November 2017
Available online 21 December 2017

Keywords:
Fiber lasers
Er
Tunable lasers
Laser dynamics
Laser instabilities
Mode instabilities

ABSTRACT

Self-swept erbium fiber laser emitting around 1.56 μm is reported in detail. Both sweep directions were registered: pointing toward longer and shorter wavelengths, redshift and blueshift sweeping, respectively. We describe method of determining the direction of the wavelength drift using the monochromator based optical spectrum analyzer. Possible root for this sweeping regime, i.e., the gain modulation along active fiber, is discussed with the help of a simple model calculating the overall cavity gain that can predict the direction of the laser wavelength sweeping.

1. Introduction

Fiber lasers become attractive sources for many applications including material processing, medicine, defense and security and their market share is rapidly increasing [1,2]. It is thanks to inherent advantages of the active medium in the form of fiber waveguide that involve excellent beam quality, high average power and wall-plug efficiency, simpler excess heat management, good and preserved overlap of the pump and signal beams [3,4]. Despite improving maturity of fiber lasers, many limiting factors have to be mitigated and also new issues emerge. Important problems currently represent different kinds of mode instabilities. Well-known is the transversal mode-instability that severely limits the fiber amplifier output power [5,6]. Another kind of instability is longitudinal mode instability that could trigger the self-Q-switched regime and they could be transformed in kind of spectra evolution characteristics. One interesting among others is the so-called spontaneous or self-induced laser line sweeping (SLLS or self-sweeping for short) regime where the laser output wavelength drifts spontaneously but almost periodically and steadily within certain spectral range. The sweeping with erbium fiber laser was not studied extensively until now and only partial results were published by our team [7,8]. We were able to distinguish both redshift and blueshift sweep directions for emitting laser line around 1.56 μm. The SLLS phenomenon in fiber lasers was briefly noticed for the first time in Ref. [9], nevertheless, only a couple of years later it was extensively studied in Refs. [10, 11]. Kir'yanov et al. described SLLS laser capability with a quite specific ytterbium fiber laser setup, using the so-called GT Wave fiber bundle as the active medium, but principally equivalent to Fabry–Perot cavity fiber laser as referred here. They achieved laser line sweeping towards longer wavelength of the spectra, here referred as normal or redshift sweeping, within an 8 nm spectral span around 1084 nm mean wavelength. Lobach et al. in Refs. [11–13] doubled the sweeping span to 16 nm and later extended to 20 nm in Ref. [14] with a commercial double clad ytterbium fiber laser setup with cavity formed by the Fresnel reflection on one end and either by fiber Bragg-grating or by fiber loop mirror on the second end. They also gave a more detailed theoretical study on SLLS; they predicted that SLLS incorporates only one or very few longitudinal modes, and assumed the square root dependence of the sweeping rate on the average laser power and sweeping rate linear decrease with cavity length.

It is commonly believed that SLLS appears in low Q cavities [10,12,14] and in cavities where very low feedback for a small portion of laser signal exists to create a standing wave inside the fiber laser cavity [15]. The theory of SLLS in solid state lasers firstly proposed in Ref. [16] was later adapted to fiber lasers in Ref. [12]. The SLLS is a phenomenon accompanied by a transient effect called relaxation oscillations appearing as long as the equilibrium state

* Corresponding author at: HiLASE Centre, Institute of Physics of the Czech Academy of Sciences, Za Radnici 828, 252 41 Dolni Brezany, Czechia.
E-mail address: navratil@fzu.cz (P. Navratil).

https://doi.org/10.1016/j.opelre.2017.11.004
1230-3402/

for inversion and laser intensity establishes. Nevertheless, several additional conditions must be fulfilled to settle the SLLS, above all, laser resonator feedback must not be single-frequency selective, thus, the resonator supports operation of plenty laser modes. With this condition also another one is linked, it is the necessity of a wide-spreading gain curve to feed the modes supported by laser cavity. Based on these conditions, crossing the threshold level for lasing, longitudinal mode with highest gain starts to be amplified and thanks to the resonator feedback a standing wave is established in the cavity. In the modes of the wave, the population inversion of excited states is depleted, thus the mode exhaust the gain for itself and may no longer be the mode with highest gain and ceases to exist. Thus, the power of another longitudinal mode whose overlap with the cavity gain areas is not perfect but still better than for the previously lasing one can rise. This procedure is repeating but in every moment only one or very few modes lase instantaneously [17]. Every longitudinal mode has a frequency defined by the length of the cavity, mode number and speed of its propagation inside the cavity. Therefore, the central frequency of the laser line in SLLS regime is moving. The mode-hopping occurs in one direction as long as the mode encounters higher gain. After that, the laser line jumps to its original position. In Ref. [10], the mechanism that propels the sweeping of the laser line towards the longer wavelengths of the spectra is explained by the dependence of gain peak wavelength on the population inversion. The peak of the gain curve in ytterbium lasers tends towards the shorter wavelengths of the spectra when increasing the population inversion [18]. Based on this property the decrease of inversion is accompanied with a gain curve peak movement towards longer wavelengths of the spectra. And this is the reason for laser line sweeping direction selection; moreover, this explains laser power decrease during wavelength passage through the sweeping span. The determination of the sweeping direction can be influenced also by the refractive index modulation and fiber Bragg gratings created in the SLLS laser cavity and their reflectivity as it was reported in the literature recently [17,19,20].

Regarding wavelength range of the self-swept lasers, several active media and corresponding wavelength ranges were demonstrated. The first reports dealt with self-swept ytterbium fiber lasers near 1.06–1.09 μm [9–11,15]. Different active medium sweeping represents [21] with linear cavity in thulium-emission range around 1.9–1.93 μm and sweeping span up to 15 nm. Lobach et al. in Ref. [22] used bismuth active fiber to achieve sweeping between 1.456 and 1.466 μm. Self-swept holmium fiber laser at around 2.1 μm is so far the latest extension of the wavelength range covered by the SLLS fiber lasers [23,24].

In this paper we report on erbium fiber laser emitting around 1.56 μm with focus on the wavelength self-sweeping operation of this fiber laser. Preliminary results of this fiber laser have been briefly presented earlier in conferences papers [7,8]. We are discussing the detailed experimental and theoretical investigation of the first self-swept erbium fiber laser. Possible root for this sweeping regime is discussed with the help of a simple model calculating the overall cavity gain that can predict the direction of the laser wavelength sweeping.

2. Experiment

We built a fiber laser including saturable absorber formed by the thulium-doped single-mode fiber from Institute of Photonics and Electronics (model No. SG1155) with peak absorption at 1.655 μm of 48.5 dB/m and absorption at 1.56 μm of 17.6 dB/m. Erbium-doped single mode fiber OFS-Fitel (model No. EDF-HG980), with peak absorption of about 13 dB/m was used as an active lasing medium. Above mentioned fibers were separated by wavelength division multiplexer (WDM) and tunable band-pass filter. The WDM coupled 980 nm pump power from single-mode laser diode EM4 (model No. PNTX-9000-A-250-976) to the active lasing medium. The tunable band-pass filter Koshin-Kogaku (model No. FC-1560B-1-3) had 3.0 nm pass band and tuning region 1.54–1.57 μm. The transmission spectra for several settings of the filter are depicted in Fig. 2. Applied to bare fiber between filter and saturable absorber was polarization controller (PC) based on rotatable fiber squeezer. Second end of the erbium-doped fiber was spliced to a 10/90 single mode fiber coupler that decoupled 10% of the intracavity power for detection. The laser resonator was established by 3.5% reflection from perpendicularly cleaved fiber ending at side of the active fiber and by fiber loop mirror (FLM) formed by a 50/50 single mode fiber coupler enabling 100% reflection at the saturable absorber side. Described fiber laser setup is sketched in Fig. 1.

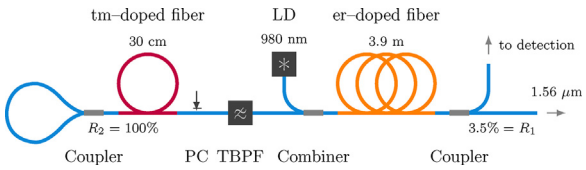

Fig. 1. Fiber laser setup with erbium-doped active medium.

The erbium-doped fiber had length of 3.9 m while the thulium-doped was only 33 cm long. Signal single mode fiber of the combiner and filter had length of 2.0 m. The two couplers forming the cavity interfaces added another 2 m. Summarizing, the whole length of the cavity for 1.56 μm signal was formed by single mode fibers only and amounts totally 8 m.

The optical spectra analyzer (OSA) ANDO (model No. AQ-1425) scans the spectra for the used resolution 0.1 nm with scanning speed $u = 1.04\ \mathrm{nm\,s^{-1}}$. The OSA can operate even in the power meter regime where the spectrometer monochromator is set to desired wavelength while the analyzer collects the time sequence within run time interval of 44 s. Digital oscilloscope Rigol (model No. DS1052E) with 50 MHz bandwidth recorded oscillations by means of an InGaAs biased detector.

The thulium-doped fiber was intended as a passive Q-switch. Unfortunately, the fiber never acted like a saturable absorber to achieve giant pulses – the fiber exhibited lower saturation intensity then we expected and only self-pulsing was attained instead. But the self-pulsing that is an accompanying effect of the SLLS phenomenon was settled and well observed. We examined simplified fiber setups by omitting one or more fiber components from the setup (Fig. 1) but none exhibited the SLLS. Moreover, the presented setup manifested the SLLS only for specific combinations of adjustment of polarization controller and selection of tunable filter transmission region. Selected recorded spectra can be seen in Fig. 2. Still, both sweep directions were registered thanks to broad setting capability. Two examples of the sweeping are presented within the paper. Therefore, the thulium-doped fiber probably played important role to observe the SLLS with erbium fiber laser as it might modify the overall cavity gain spectral characteristics. However, the spatial hole burning effect probably did not happen in the thulium fiber as it was the case in the erbium fiber because the signal laser power in the thulium fiber was only several mW and excited population of thulium ions was negligible.

3. Results

Immediate assignment between measured characteristics and sweep direction was impossible; suitable measurement device for recording swept laser line dynamics directly was not available for the measurements. We applied data analysis to discover the sweep

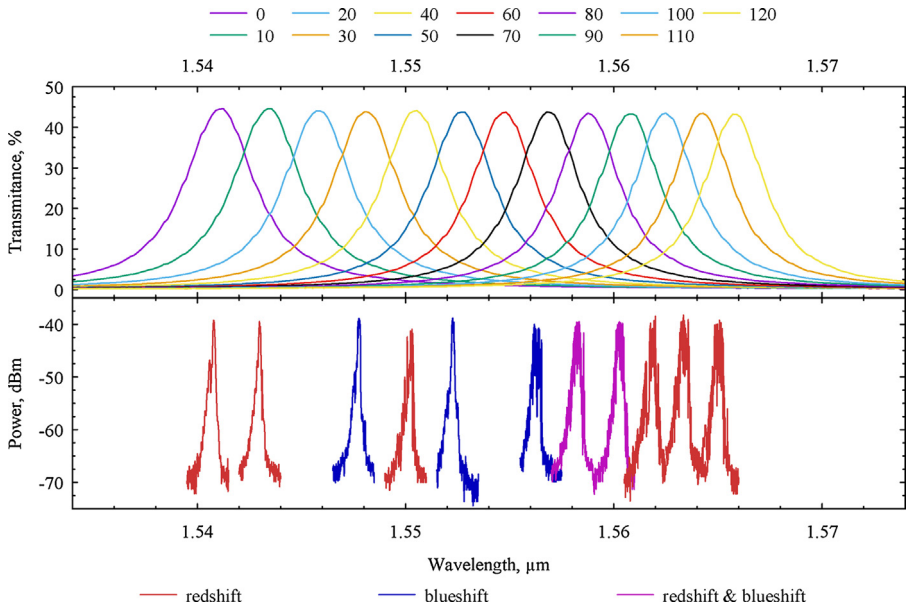

Fig. 2. Transmission spectra of the tunable band-pass filter Koshin-Kogaku (upper subset) and emission spectra of the erbium fiber laser (lower subset) for several settings of the filter. Colors are to indicate the sweep directions.

direction displayed by recorded data. Hereinafter, dependencies belonging to redshift sweeping (r) and blueshift sweeping (b) are to be viewed respectively in upper and lower subsets of displayed graphs.

Following sweeping results were achieved for tunable filter setting permitting lasing around 1.559 μm. By the adjustment of the PC we were able to control the direction of the sweeping. An example of power time evolution of several sweeping periods and detail of pulse sequence respectively is given in Fig. 3(a) and 3(b). In order to establish the sweep period

$$\tau^{(r)} = 130 \text{ ms}, \qquad \tau^{(b)} = 290 \text{ ms},$$

we analyzed set of oscillograms belonging to the same PC adjustment.

Sweeping is demonstrated by comb-like spectrograms in Fig. 4(a) . The set of spectrograms belonging to one PC adjustment was analyzed to achieve the sweep range and span

$$\Lambda^{(r)} = 0.37 \text{ nm}; \qquad \Lambda^{(b)} = 0.43 \text{ nm},$$

and to calculate the peak to peak spectral distance $\delta\lambda$ and, consequently, periods $\tau^{(r)}$, $\tau^{(b)}$ for proofing of the sweep direction. In Fig. 4(b), the time evolution of optical power at a wavelength of 1.559 μm is shown. In this case, the OSA was set to power meter mode at fixed wavelength. Again, periods $\tau^{(r)}$, $\tau^{(b)}$ were calculated and they correspond to the values read from Fig. 3(a).

Detailed explanation of data analysis with intention to distinguish redshift and blueshift sweeping follows. The interval τ is a time elapsed between two following peaks appearing in spectrogram measurement at distance $\delta\lambda$ and could be related to OSA scanning speed u, laser line sweep span Λ, and sweep rate v through:

$$\tau = \frac{\delta\lambda}{u} = \frac{\Lambda \pm \delta\lambda}{v}. \tag{1}$$

First way is to express the interval τ from the OSA scanning speed u, the second way engages the sweep rate v. In the case of redshift sweeping, the laser line passes through the wavelength sweep span Λ enlarged by an increment $\delta\lambda^{(r)}$ at the speed of line sweep velocity $v^{(r)}$ (+ sign applied). In the blueshift sweeping case, where laser line sweeps at the speed of $v^{(b)}$, the line does not pass the whole sweep span Λ but just a part reduced by decrement $\delta\lambda^{(b)}$ (− sign). See Fig. 5 for better understanding.

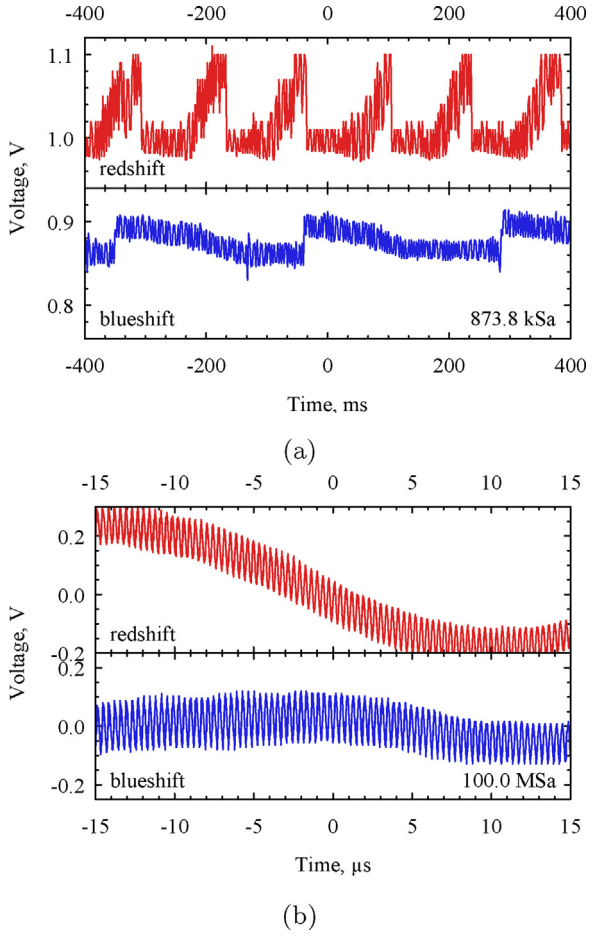

Fig. 3. Oscillograms for redshift (upper subsets) and blueshift (lower subsets) sweeping for self-swept erbium laser set to wavelength of 1.559 μm by the Koshin-Kogaku filter.

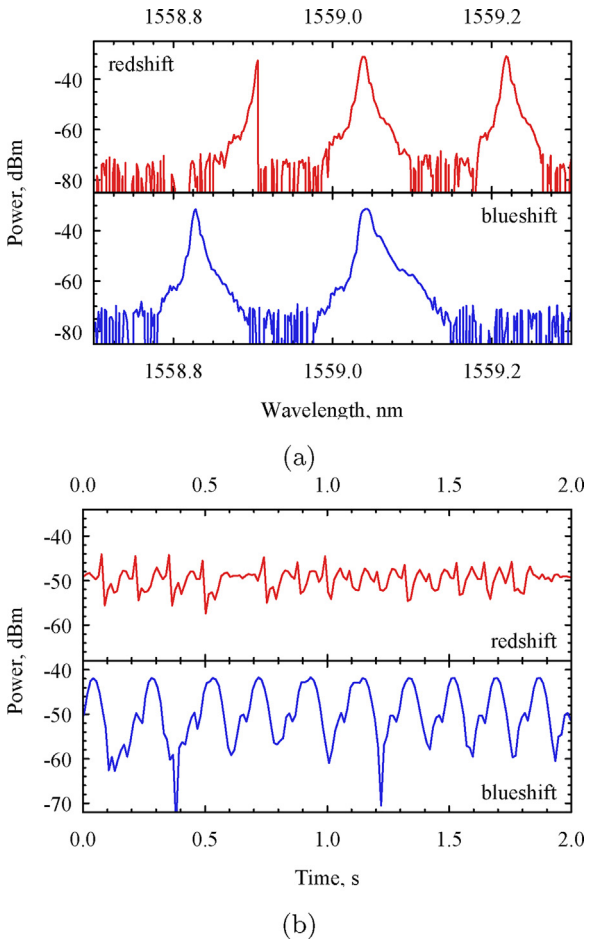

Fig. 4. (a) Spectrograms and (b) time evolution at a wavelength of 1559.0 nm for redshift (upper subsets) and blueshift (lower subsets) sweeping for self-swept erbium laser set to wavelength of 1.559 μm by the Koshin-Kogaku filter.

From Eq. (1), we can express the distance:

$$\delta\lambda^{(r)} = \frac{\Lambda^{(r)} u}{v^{(r)} - u} \tag{2}$$

for the redshift sweeping; and, on the contrary, for blueshift sweeping:

$$\delta\lambda^{(b)} = \frac{\Lambda^{(b)} u}{v^{(b)} + u}. \tag{3}$$

We have performed simultaneous measurement of spectra and time evolutions, that means we have a set of oscillograms corresponding to a set of spectrograms for both sweep directions. If we accept already mentioned assignment that upper oscillograms (Fig. 3) and spectrogram (Fig. 4) matches to redshift sweeping and lower to blueshift sweeping we could exploit already calculated spans ($\Lambda^{(r)}$, $\Lambda^{(b)}$) and intervals ($\tau^{(r)}$, $\tau^{(b)}$) to compute redshift and blueshift sweep rates

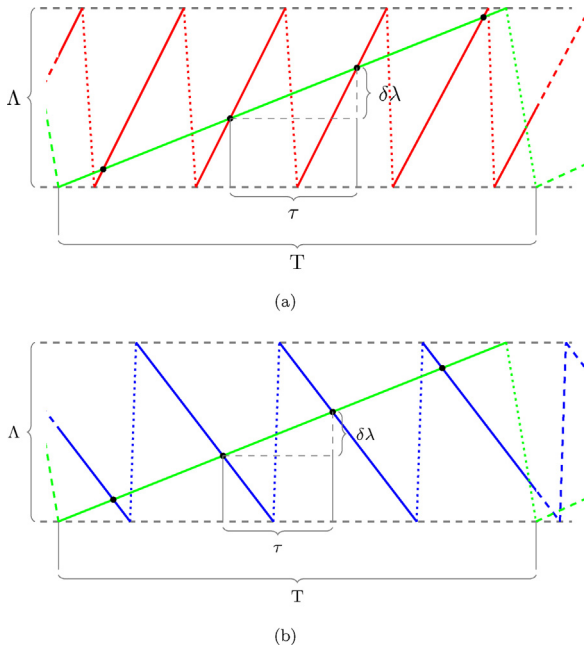

Fig. 5. Illustration to the proof of (a) redshift and (b) blueshift sweeping. Green line is to illustrate the OSA scanning, other color lines are to illustrate the laser line sweeping.

$$v^{(r)} = \frac{0.37\ \text{nm}}{130\ \text{ms}} = 2.85\ \text{nm}\ s^{-1}; \qquad v^{(b)} = \frac{0.43\ \text{nm}}{290\ \text{ms}} = 1.48\ \text{nm}\ s^{-1}.$$

Finally, we can evaluate wavelength difference using Eqs. (2) and (3):

$$\delta\lambda^{(r)} = 0.21\ \text{nm}; \qquad \delta\lambda^{(b)} = 0.18\ \text{nm}.$$

If we assume opposite assignment that upper oscillograms (Fig. 3) and spectrogram (Fig. 4) matches to blueshift sweeping and lower to redshift sweeping, we should find a disagreement between calculated and measured data. In this case, wavelength increments equal:

$$\delta\lambda^{(r)} = 1.02\ \text{nm}; \qquad \delta\lambda^{(b)} = 0.10\ \text{nm},$$

but these are not in accordance with measured data:

$$\delta\lambda^{(r)} = (0.15 \pm 0.02)\ \text{nm}$$

$$\delta\lambda^{(b)} = (0.197 \pm 0.008)\ \text{nm}.$$

Sweeping parameters related to redshift and blueshift sweep regimes are to be viewed in Table 1.

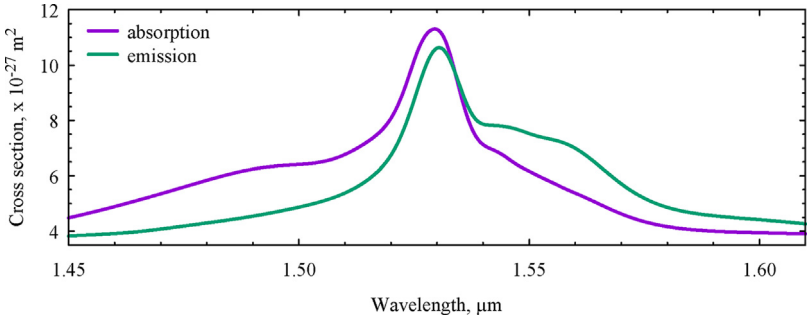

Fig. 6. Emission and absorption cross-section of the erbium-doped fiber of similar composition as used in the experiment.

Table 1
Sweep parameters for self-swept erbium laser set to wavelength of 1.559 μm by the Koshin-Kogaku filter. Sweep rate is an averaged swept laser line velocity.

Sweeping	Range (nm)	Span (nm)	Period (ms)	Rate (nm s^{-1})
Redshift	1558.90–1559.27	0.37	130	2.85
Blueshift	1558.76–1559.19	0.43	290	1.48

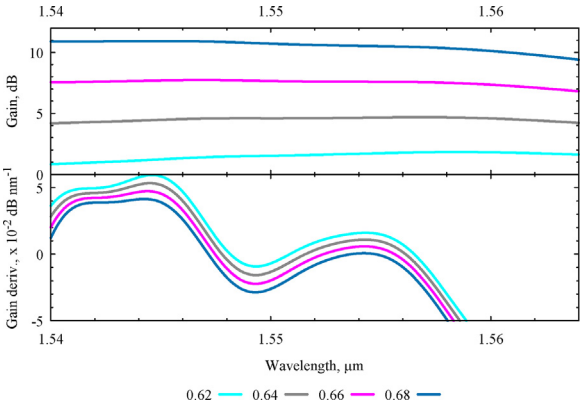

Fig. 7. Calculated spectra of gain (upper subset) and its first derivative with respect to wavelength (lower subset) for several values of relative population on the metastable level.

4. Discussion

There are two approaches to explain the determination of sweep direction, both were discussed in our previous work [25], thus, only short explanation will be presented. The temporal wavelength dynamics of a self-swept laser is related to spatial hole burning. The burning affects the appearing of the spatial gain grating and coupled spatial phase grating discussed in the introduction.

One approach assumes that spatial gain grating is the key effect and mechanism predetermining sweep direction is a gain curve dependence. If a hole in the shape of the sinc function is burnt into the gain curve maximum than the inclination of the hole surroundings determines which of the two sinc lobes will be higher. Naturally, the lobe at the side of milder gain curve inclination has higher gain value and predetermines the movement direction. Both possibilities – redshift and blueshift sweep directions – are illustrated respectively in upper and lower sub-figure (Fig. 8). The model is based on the calculation of the active medium length averaged gain [26] which is depicted in Fig. 7 and come out of the cross-section of the erbium-doped fiber from Fig. 6. The values of the cross-section are not given for the real erbium-doped fiber used in the experiment but of an erbium-doped fiber of similar composition.

In the second approach, the wavelength dynamics is predetermined by the phase grating. The model [17] predicts that the refractive index grating produced by actual lasing mode suppresses the existence of the mode itself. It was proofed [19,20] that the grating has a maximum reflectivity detuned from the lasing mode. Next created mode wavelength depends on the evolution of the grating reflectivity function. Whether the model predicts the next maximum reflectivity moved towards longer wavelength – the lasing mode wavelength will move accordingly and vice versa.

5. Conclusions

We have reported for the first time in detail the observations of the self-induced laser line sweeping in the erbium fiber laser. The laser emission was tunable within the broad spectral range of 1.54–1.57 μm by using a pigtailed tunable filter. The sweeping in both directions was registered, i.e., we observed sweeping either towards longer (redshift sweeping) or shorter (blueshift sweeping) wavelengths of the spectra depending on the settings of the tunable filter and polarization controller. Since direct indication of the sweeping direction was not available, we have shown proof of the direction of sweeping from the dynamic spectra recordings and from the oscillograms of the output power. We described a semiempirical model based on the gain curve spectra that can explain predetermination of the sweep direction.

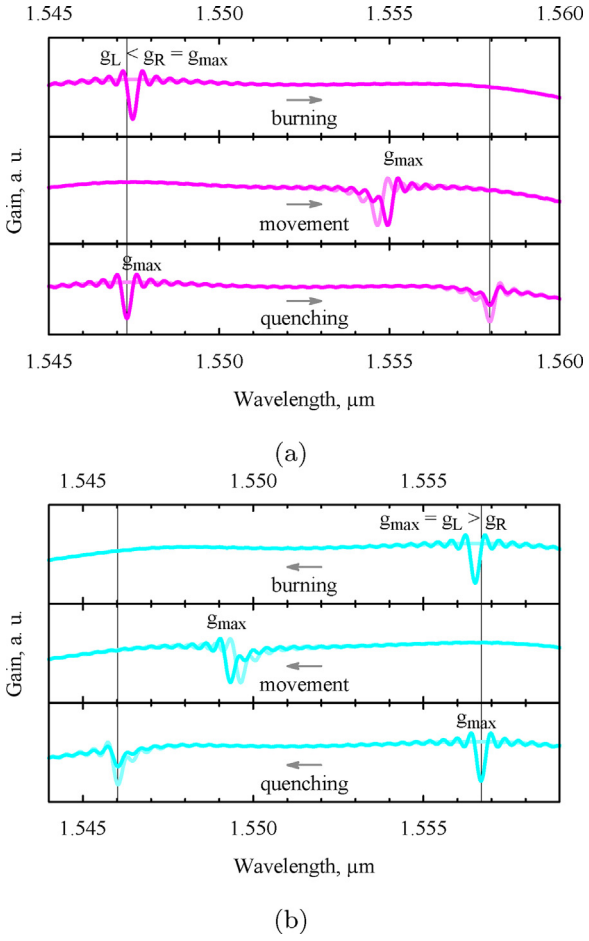

Fig. 8. Modeled gain spectra evolution for (a) redshift and (b) blueshift sweeping.

Acknowledgements

The research was supported by the Czech Science Foundation under project No. 16-13306S and by the Czech Ministry of Education, Youth and Sports under project No. SGS16/247/OHK4/3T/14.

References

[1] S. Taccheo, K. Schuster, M. Ferrari, A. Seddon, M. Marciniak, C. Taudt, J. Troles, G. Valentini, D. Dorosz, F. Prudenzano, M. Jaeger, C. Dandrea, M. Ivanda, A. Chiasera, S. Sujecki, V. Nazabal, D. Comelli, H. Baghdasaryan, T. Baselt, P. Hartmann, A. Lucianetti, P. Peterka, A. Klotzbach, J.L. Adam, H. Gebavi, Challenges and future trends in fiber lasers, 2016 18th International Conference on Transparent Optical Networks (ICTON) (2016) 1–5, http://dx.doi.org/10.1109/ICTON.2016.7550715.
[2] J. Sotor, M. Pawliszewska, G. Sobon, P. Kaczmarek, A. Przewolka, I. Pasternak, J. Cajzl, P. Peterka, P. Honzátko, I. Kašík, W. Strupinski, K. Abramski, All-fiber Ho-doped mode-locked oscillator based on a graphene saturable absorber, Opt. Lett. 41 (11) (2016) 2592–2595, http://dx.doi.org/10.1364/OL.41.002592 http://ol.osa.org/abstract.cfm?URI=ol-41-11-2592.
[3] M. Michalska, W. Brojek, Z. Rybak, P. Sznelewski, M. Mamajek, J. Swiderski, Highly stable, efficient Tm-doped fiber laser – a potential scalpel for low

invasive surgery, Laser Phys. Lett. 13 (11) (2016) 115101 http://stacks.iop.org/1612-202X/13/i=11/a=115101.
[4] P. Peterka, P. Honzatko, I. Kasik, O. Podrazky, F. Todorov, J. Cajzl, P. Koska, Y. Baravets, J. Aubrecht, J. Mrazek, Thulium-doped fibers and fiber-optic components for fiber lasers at around 2 μm, Fine Mechanics and Optics 60 (5–6) (2015) 174–177.
[5] C. Jauregui, H.-J. Otto, S. Breitkopf, J. Limpert, A. Tünnermann, Optimizing high-power Yb-doped fiber amplifier systems in the presence of transverse mode instabilities, Opt. Express 24 (8) (2016) 7879–7892, http://dx.doi.org/10.1364/OE.24.007879 http://www.opticsexpress.org/abstract.cfm?URI=oe-24-8-7879.
[6] M.N. Zervas, Transverse mode instability analysis in fiber amplifiers, Proc. SPIE 10083 (2017), http://dx.doi.org/10.1117/12.2252435, 100830M-100830M-9.
[7] P. Honzatko, P. Vojtisek, P. Navratil, P. Peterka, Self-induced laser line sweeping in tunable erbium-doped fiber laser, Proc. 5th EPS-QEOD Europhotonics Conf. (2013).
[8] P. Peterka, P. Navratil, B. Dussardier, R. Slavik, P. Honzatko, V. Kubecek, Self-induced laser line sweeping and self-pulsing in double-clad fiber lasers in Fabry-Perot and unidirectional ring cavities, Proc. SPIE 8433 (2012), http://dx.doi.org/10.1117/12.924298, 843309-1-843309-8.
[9] P. Peterka, J. Maria, B. Dussardier, R. Slavik, P. Honzatko, V. Kubecek, Long-period fiber grating as wavelength selective element in double-clad Yb-doped fiber-ring lasers, Laser Phys. Lett. 6 (2009) 732–736.
[10] A. Kir'yanov, N. Il'ichev, Self-induced laser line sweeping in an ytterbium fiber laser with non-resonant Fabry-Perot cavity, Laser Phys. Lett. 8 (2011) 305–312.
[11] I.A. Lobach, S.A. Babin, S.I. Kablukov, E.V. Podivilov, Broad-range self-sweeping of a narrow-line Yb-doped fiber laser, in: Proc. 20th International Laser Physics Workshop (LPHYS'11), vol. 8.1.4, Sarajevo, Bosnia and Herzegovina, 2011.
[12] I.A. Lobach, S.I. Kablukov, E.V. Podivilov, S.A. Babin, Broad-range self-sweeping of a narrow-line self-pulsing Yb-doped fiber laser, Opt. Express 19 (2011) 17632–17640.
[13] I.A. Lobach, S.I. Kablukov, E.V. Podivilov, S.A. Babin, All-fiber broad-range self-sweeping Yb-doped fiber laser, Proc. SPIE 8237 (2012), 82371C-1–82371C-7.
[14] I.A. Lobach, S.I. Kablukov, Application of a self-sweeping Yb-doped fiber laser for high-resolution characterization of phase-shifted FBGs, J. Lightwave Technol. 31 (18) (2013) 2982–2987.
[15] P. Peterka, P. Navratil, J. Maria, B. Dussardier, R. Slavik, P. Honzatko, V. Kubecek, Self-induced laser line sweeping in double-clad Yb-doped fiber-ring lasers, Laser Phys. Lett. 9 (2012) 445–450.
[16] V.V. Antsiferov, V.S. Pivtsov, V.D. Ugozhaev, K.G. Folin, Spike structure of the emission of solid-state lasers, Sov. J. Quantum Electron. 3 (3) (1973) 211–215.
[17] I.A. Lobach, S.I. Kablukov, E.V. Podivilov, S.A. Babin, Self-scanned single-frequency operation of a fiber laser driven by a self-induced phase grating, Laser Phys. Lett. 11 (2014) 1–6.
[18] H.M. Pask, R.J. Carman, D.C. Hanna, A.C. Tropper, C.J. Mackechnie, P.R. Barber, J.M. Dawes, Ytterbium-doped silica fiber lasers: versatile sources for the 1–1.2 μm region, IEEE J. Sel. Topics Quantum Electron. 1 (1) (1995) 2–13, http://dx.doi.org/10.1109/2944.468377.
[19] P. Peterka, P. Honzatko, P. Koska, F. Todorov, J. Aubrecht, O. Podrazky, I. Kasik, Reflectivity of transient Bragg reflection gratings in fiber laser with laser-wavelength self-sweeping, Opt. Express 22 (24) (2014) 30024–30031, http://dx.doi.org/10.1364/OE.22.030024 http://www.opticsexpress.org/abstract.cfm?URI=oe-22-24-30024.
[20] P. Peterka, P. Honzatko, P. Koska, F. Todorov, J. Aubrecht, O. Podrazky, I. Kasik, Reflectivity of transient Bragg reflection gratings in fiber laser with laser-wavelength self-sweeping: erratum, Opt. Express 24 (24) (2016) 16222–16223.
[21] X. Wang, P. Zhou, X. Wang, H. Xiao, L. Si, Tm-Ho co-doped all-fiber brand-range self-sweeping laser around 1.9 μm, Opt. Express 21 (14) (2013) 16290–16295.
[22] I.A. Lobach, S.I. Kablukov, M.A. Melkumov, V.F. Khopin, S.A. Babin, E.M. Dianov, Single-frequency bismuth-doped fiber laser with quasi-continuous self-sweeping, Opt. Express 23 (19) (2015) 24833–24842, http://dx.doi.org/10.1364/OE.23.024833 http://www.opticsexpress.org/abstract.cfm?URI=oe-23-19-24833.
[23] J. Aubrecht, P. Peterka, P. Koska, O. Podrazký, F. Todorov, P. Honzátko, I. Kašík, Self-swept holmium fiber laser near 2100 nm, Opt. Express 25 (4) (2017) 4120–4125, http://dx.doi.org/10.1364/OE.25.004120 http://www.opticsexpress.org/abstract.cfm?URI=oe-25-4-4120.
[24] J. Aubrecht, P. Peterka, P. Koska, P. Honzatko, M. Jelinek, M. Kamradek, M. Frank, V. Kubecek, I. Kasik, Spontaneous laser-line sweeping in Ho-doped fiber laser, Proc. SPIE 10083 (2017), http://dx.doi.org/10.1117/12.2249486, 100831v-100831V-6.
[25] P. Navratil, P. Peterka, P. Honzatko, V. Kubecek, Reverse spontaneous laser line sweeping in ytterbium fiber laser, Laser Phys. Lett. 14 (3) (2017) 035102 http://stacks.iop.org/1612-202X/14/i=3/a=035102.
[26] C.R. Giles, C.A. Bums, D.J. DiGiovanni, N.K. Dutta, G. Raybon, Characterization of erbium-doped fibers and application to modeling 980 nm and 1480 pumped amplifiers, IEEE Photon. Technol. Lett. 3 (4) (1991) 363–365.